Journal of Visualized Experiments

Real-time monitoring of Aurora kinase A activation using conformational FRET biosensors in live cells.

--Manuscript Draft--

Article Type:	Invited Methods Article - JoVE Produced Video
Manuscript Number:	JoVE61611R1
Full Title:	Real-time monitoring of Aurora kinase A activation using conformational FRET biosensors in live cells.
Section/Category:	JoVE Biology
Keywords:	AURKA; FRET; FLIM; genetically-encoded biosensors; conformational change; activation; mitosis; live cells
Corresponding Author:	Giulia Bertolin, PhD Centre National de la Recherche Scientifique Rennes cedex, France FRANCE
Corresponding Author's Institution:	Centre National de la Recherche Scientifique
Corresponding Author E-Mail:	giulia.bertolin@univ-rennes1.fr
Order of Authors:	Giulia Bertolin, PhD
	Gilles Le Marchand
	Marc Tramier
Additional Information:	
Question	**Response**
Please indicate whether this article will be Standard Access or Open Access.	Open Access (US$4,200)
Please indicate the **city, state/province, and country** where this article will be **filmed**. Please do not use abbreviations.	Rennes, France

Dr. Alisha DSouza
Senior review editor
JoVE editorial board
Rennes, 17th June, 2020

UMR 6290 CNRS – UR1
igdr.univ-rennes1.fr
Faculté de Médecine
2 avenue du Professeur Léon Bernard
35043 Rennes cedex, France
giulia.bertolin@univ-rennes1.fr
T. +33 (0)2 23 23 75 16
F. +33 (0)2 23 23 44 78

Dear Dr. DSouza,

Thank you again for evaluating our work, and for giving us the opportunity to provide further information to reinforce the strength of our findings. Please find enclosed our revised manuscript entitled "*Real-time monitoring of Aurora kinase A activation using conformational FRET biosensors in live cells*" by Giulia Bertolin *et al*.

We appreciated the reviewers' comments, thanks to which our manuscript has been greatly improved. As you will see in our point-by-point response, we have carefully addressed each of their concerns with two updated figures (Figs. 1 and 4) and more extensive explanations in the main text. We also corrected the manuscript where appropriate, always according to the rewievers' suggestions.

All the new elements provided in this second version of the manuscript are now labelled in blue within the main text. We are confident that you and the reviewers will find in our revised manuscript convincing answers in response to the key points raised.

Last, we carefully addressed all the editorial comments requested in your email, and we hope that they will make our manuscript closer to the style suitable for the publication of our full-length written protocol in *JoVE*.

We hope that our manuscript will now be deemed suitable for publication, and we look forward to hearing from you in the near future.

Yours sincerely,

Giulia Bertolin, Ph.D.

TITLE:

Real-Time Monitoring of Aurora kinase A Activation using Conformational FRET Biosensors in Live Cells

AUTHORS AND AFFILIATIONS:

Giulia Bertolin, Gilles Le Marchand, Marc Tramier

Univ Rennes, CNRS, IGDR (Genetics and Development Institute of Rennes), UMR 6290, Rennes, France

giulia.bertolin@univ-rennes1.fr
gilles.le-marchand@univ-rennes1.fr
marc.tramier@univ-rennes1.fr

CORRESPONDING AUTHORS:

Giulia Bertolin (giulia.bertolin@univ-rennes1.fr)
Marc Tramier (marc.tramier@univ-rennes1.fr)

KEYWORDS:

AURKA, FRET, FLIM, genetically-encoded biosensors, conformational change, activation, mitosis, live cells.

SUMMARY:

The activation of the multifunctional Ser/Thr kinase AURKA is hallmarked by its autophosphorylation on Thr288. Fluorescent probes relying on FRET can discriminate between its inactive and activated states. Here, we illustrate some strategies for probe engineering, together with a rapid FRET protocol to follow the kinase activation throughout mitosis.

ABSTRACT:

Epithelial cancers are often hallmarked by the overexpression of the Ser/Thr kinase Aurora A/AURKA. AURKA is a multifunctional protein that activates upon its autophosphorylation on Thr288. AURKA abundance peaks in mitosis, where it controls the stability and the fidelity of the mitotic spindle, and the overall efficiency of mitosis. Although well characterized at the structural level, a consistent monitoring of the activation of AURKA throughout the cell cycle is lacking. A possible solution consists in using genetically-encoded Förster's Resonance Energy Transfer (FRET) biosensors to gain insight into the autophosphorylation of AURKA with sufficient spatiotemporal resolution. Here, we describe a protocol to engineer FRET biosensors detecting Thr288 autophosphorylation, and how to follow this modification during mitosis. First, we provide an overview of possible donor/acceptor FRET pairs, and we show possible cloning and insertion methods of AURKA FRET biosensors in mammalian cells. Then, we provide a step-by-step analysis for rapid FRET measurements by fluorescence lifetime imaging microscopy (FLIM) on a custom-built setup. However, this protocol is also applicable to alternative commercial solutions available. We conclude by considering the most appropriate FRET controls for an AURKA-based biosensor, and by highlighting potential future improvements to further increase

the sensitivity of this tool.

INTRODUCTION:

Aurora kinase A/AURKA is a multifunctional serine/threonine kinase, active throughout the cell cycle and at different subcellular compartments[1]. Understanding its broad spatiotemporal activation is particularly important in cancer, as AURKA is often overexpressed in epithelial and hematological malignancies, with patients showing poor responsiveness to the currently available therapies [2].

Structural studies revealed that AURKA undergoes two steps to convert from an inactive to an active kinase. First, the autophosphorylation of Thr288 changes the conformation of the kinetic pocket of the kinase and activates it[3–6]. This step increases the catalytic activity of AURKA in human cells and in *Xenopus laevis*[3,6,7], priming the kinase for full activity. Once activated, the interaction of AURKA with the targeting protein for Xklp2 (TPX2) induces a second conformational change[5]. This further modification allows AURKA to reach full enzymatic activity towards its substrates in the cell[5,8–10].

For nearly two decades, insights on the activation and activity of AURKA were obtained mainly through a combination of biochemical approaches. These include the detection of phosphorylated Thr288 in cells or in vivo as a hallmark of AURKA activation, crystallographic analyses, and in vitro or in cellulo kinase assays to probe the activity of AURKA[1]. However, the spatiotemporal resolution of these approaches is poor or absent, and novel solutions were needed to broaden the knowledge of the dynamics of these two events.

The development of fluorescent probes in the last few years facilitated the monitoring of AURKA in live cells, allowing the following of its activation with greater spatiotemporal resolution. The most specific sensors for AURKA developed so far rely on the FRET principle (Förster's Resonance Energy Transfer)[11] to discriminate between inactive and active (autophosphorylated) AURKA. The first sensor developed was a substrate-based biosensor of AURKA kinase activity. Substrate-based biosensors are constituted by a short aminoacidic sequence targeted by a given kinase for phosphorylation, and inserted within a donor/acceptor FRET pair and a binding domain recognizing the phosphorylated residue, which helps the folding of the biosensor for an efficient FRET process[12]. In the case of AURKA, a 14-aminoacid fragment of KIF2C targeted by phosphorylation was inserted between a CFP-YFP donor/acceptor pair[13]. However, this sensor has some major drawbacks. First, the KIF2C sequence used in this probe can be targeted both by AURKA and the closely-related kinase AURKB, thereby decreasing the specificity of this biosensor. Second, the sensor relies on the endogenous kinase for phosphorylation. Therefore, FRET efficiency can be undetectable or not significant if the quantities of the kinase are limiting (e.g., in subcellular compartments or cell cycle phases). To overcome these limitations, a new class of AURKA sensor was created known as "conformational sensors". In these probes, the full-length sequence of AURKA was inserted within a donor fluorophore at the N-terminus, and an acceptor fluorophore at the C-terminus. Inactive AURKA presents an "open" conformation, which brings the N- and C-termini of the kinase away from each other. With such distance between the two termini (> 10 nm), the donor/acceptor pair are at a non-permissive configuration for FRET. On

the contrary, autophosphorylated AURKA adopts a "closed" conformation, with the two protein termini and the two fluorophores in proximity. This was shown to allow FRET between the donor and the acceptor, which can be measured using the variations in the donor lifetime[14,15]. Such probes present several advantages. First, they are genetically-encoded, and they can be used to replace the endogenous kinase in the cell. Second, they rescue the phenotypes induced by the knockdown of AURKA, indicating that they are functional in the cell. Third, they allow to follow the activation of the kinase at different subcellular compartments and throughout the cell cycle. The probes detected the activation of AURKA at locations where the kinase is known to be activated (i.e. centrosomes and the mitotic spindle), and also participated in discovering the activation of AURKA at the mitochondria[16]. Last, these sensors allowed high-content screenings based on FRET/FLIM, where the conformational changes of AURKA were used to identify novel pharmacological inhibitors[17].

In the present work, we describe a procedure to visualize AURKA activation in cultured cells. First, we will make an insight on potential fluorophore pairs for FRET. The choice of the most suitable donor/acceptor pair will be made according to the available microscope setup, or a particular downstream application as multiplex FRET[18,19]. Then, we propose a pipeline to explore the behavior of the biosensor(s) chosen in a rapid FRET/FLIM microscope setup. This pipeline will extend from cell culture and synchronization procedures to FLIM acquisition and data analysis. Last, we will discuss the potential advantages of this protocol, as an analogous strategy for biosensor design could be applied to other kinases, and it may also be used with other FRET-based imaging systems.

PROTOCOL:

NOTE: U2OS cells used in this protocol were purchased from American Type Culture Collection (ATCC, HTB-96), and they were tested free from mycoplasma. Step 2.1 to 2.7 should be performed under a laminar flow hood to keep cells and reagents sterile.

1. Choosing the donor/acceptor FRET pair

1.1 Refer to the literature for the choice of the most suitable donor/acceptor FRET pairs. Useful examples can be found in [20–24], although the final choice must be made according to the characteristics of the FRET/FLIM setup (available laser lines, filters, etc.). The following are some considerations on how to select a donor/acceptor pair.

1.1.1 Choosing the donor: refer to FP base (https://www.fpbase.org/) for a complete set of information on the available fluorescent proteins. This database is constantly updated with all the newly-developed fluorophores.

1.1.2 Refer to the Fluorescent Biosensor Database (https://biosensordb.ucsd.edu/index.php) for more information on the biosensors already available in the literature, together with the respective fluorescent proteins used.

1.1.3 As a general starting point, choose a bright donor fluorophore. Good candidates are cyan fluorescent proteins as mTFP1 or ECFP, or GFP variants as EGFP or mEGFP.

1.1.4 Oligomers can affect protein localization and/or function[25]. Consider using monomeric mutants of CFP as mTurquoise2[26], or Aquamarine[27,28]. These variants also have good quantum yield and extinction coefficients, which make them good candidates as FRET donors.

1.1.5 Give preference to fluorescent proteins (both as donor or acceptors) insensitive to environmental changes like intracellular pH[23], or to photobleaching[25], as FRET efficiency can be heavily affected by these parameters[29]. Nowadays, fluorophores like mTurquoise2 or mTFP1 are extensively used as donors, thanks to their good photostability[22,25,26].

1.2 Choosing the acceptor: cyan donors are often paired with Yellow Fluorescent Protein (YFP) variants, as mVenus, Citrine, and YPet[20–22,30]. However, it should be noted that these proteins have a much greater sensitivity to pH, and globally display a poor photostability.

1.2.1 Consider using newly-developed, pH-insensitive yellow variants of YFP as pH-Lemon[31], green fluorophores as mNeonGreen[23] or red fluorophores as mScarlet-I[23,32] as previously-validated fluorescent acceptors for mTurquoise2.

1.2.2 Alternatively, consider using non-fluorescent/dark derivatives of YFP as ShadowG[33] or ShadowY[34], which were shown to behave as good acceptors for cyan-fluorescent donors in FRET/FLIM experiments.

1.2.3 If using mEGFP as a donor, consider using monomeric red acceptors as mCherry.

1.3 Verify the spectral properties of the chosen donor/acceptor pair using the tools available on the FP base website. See **Figure 1** for an example of the mEGFP/mCherry pair.

1.3.1 On the FP base website, select the **Tools** drop-down menu and select **Spectra viewer**.

1.3.2 In the drop-down menus, enter the name of the fluorophore pair to visualize (e.g., mEGFP and mCherry).

1.3.3 Simulate the properties of the donor/acceptor pair with a specific light source by selecting a given laser in the drop-down menu. Alternatively, enter a specific laser wavelength by selecting **Add laser**. Click on the **Normalize emission to this** option to adjust the fluorophore spectra to the desired wavelength. Here, the wavelength used to excite GFP is at 480 ± 10 nm.

1.4 Clone the selected donor/acceptor pair by adding one fluorophore at the N-terminus of the full-length sequence of AURKA, and one at the C-terminus. Follow the guidelines of the preferred cloning method to insert this construct in a mammalian expression vector of choice.

2. Cell culture, transfection and synchronization

2.1 DAY 1. Prepare culture medium for U2OS cells: use Dulbecco's Modified Eagle Medium (DMEM) supplemented with 10% Fetal Bovine Serum (FBS), 1% Penicillin-Streptomycin and 1% L-Glutamine (from here on, *Complete growth media*). Alternatively, DMEM with pre-supplemented L-Glutamine can also be used.

2.2 If cells are frozen, thaw a vial at least 8 days prior to experiments (i.e., from point 2.5 on).

2.3 Grow cells in an incubator dedicated to mammalian cell cultures at 37 °C and with 5% CO_2. Clean and sterilize the incubator regularly to avoid contaminations.

2.4 When the cells reach ~80% confluence:

2.4.1. Wash them briefly with sterile 1x phosphate buffer saline (PBS) without Ca^{2+} and Mg^{2+}.

2.4.2. Trypsinize cells with sterile 0.05% Trypsin-EDTA according to manufacturer's protocol and by placing cells in the incubator for 1-3 min.

2.4.3. Inactivate trypsin by adding twice the volume of complete growth media; mix well.

2.4.4. Centrifuge the cell suspension at 800 x *g* for 3-5 min.

2.4.5. Count the cells using a hemocytometer and calculate the appropriate dilution for them to be at ~70-80% confluency in chamber slides the day after. Alternatively, similar supports for live cell imaging can also be used.

2.4.6. Pipet the corresponding volume of cells in the chosen live cell imaging support, and place cells back in the incubator until the day after.

2.5 DAY 2. Proceed with transfection. Follow the guidelines of the preferred transient transfection method(s) to obtain an optimal transfection efficiency (~50/80%). No specific transfection method is required. Note that the transfection efficiency may vary according to the cell line used. Incubate for 48 h.

NOTE: Produce stable clones containing each of the three vectors to bypass the need of transient transfections. At this stage, two types of controls should be planned. First, a "donor-only" control is required to verify that the presence of full-length AURKA does not perturb the lifetime of mTurquoise2 per se. Second, a biosensor carrying a kinase-dead mutation should be used as a negative control where FRET is abolished or significantly lowered. Alternatively to a kinase-dead mutant, a chemical inhibitor of AURKA activation as the ATP analog MLN8237 can be used as a negative control.

2.5.1 Plan ahead three transfection conditions, each of them in an independent well:
The "donor-only" vector (e.g., AURKA-mTurquoise2)

The “biosensor” (e.g., superYFP-AURKA-mTurquoise2)
A kinase-dead/”K162M” biosensor (e.g., superYFP-AURKA K162M-mTurquoise2) or alternatively, an inhibitor of AURKA activation (e.g., MLN8233)

2.5.2 Carry out three conditions for each independent donor/acceptor pair to compare.

2.5.3 Consider doubling the number of transfected wells if comparing unsynchronized and G2/M-synchronized cells (see step 2.6).

2.6 DAY 3. Synchronize cells in G2/M. Add 100 ng/mL nocodazole dissolved in DMSO to each transfected well avoiding light exposure and incubate for 16 h (preferably overnight). If comparing unsynchronized and G2/M-synchronized cells, treat each transfection condition with nocodazole or with an equal volume of DMSO. For a better synchronization efficiency, prepare single-use aliquots of nocodazole in DMSO, store them at -20 °C and discard them after use.

NOTE: Cell synchronization efficiency can vary among cell lines. The optimal concentration of nocodazole and its incubation time should be experimentally determined by flow cytometry approaches prior to FRET/FLIM experiments. For statistically relevant FRET/FLIM analyses, we recommend a synchronization efficiency in G2/M of at least 50% of the overall cell population.

2.7 DAY 4. Nocodazole washout and FRET/FLIM imaging on mitotic cells

2.7.1 Remove the culture medium with a pipette and replace it with pre-warmed, sterile PBS. Avoid light exposure if possible. Gently rock the plate.

2.7.2 Repeat the washing procedure, always avoiding light exposure.

2.7.3 Remove the second PBS washing and replace it with pre-warmed, sterile Leibovitz L-15 medium, supplemented with 20% Fetal Bovine Serum (FBS) and 1% Penicillin-Streptomycin (from here on imaging media).

NOTE: Imaging media should be purchased without pH indicators (e.g., phenol red) and medium components as riboflavin. These substances are a source of autofluorescence that could perturb lifetime values.

2.7.4 Proceed with FRET/FLIM imaging. Minimize rapid changes in temperature and proceed to the imaging step (step 3) as fast as possible. Consider protecting the sample from light while transporting it to the microscope setup (i.e., by wrapping it in an aluminum foil or placing it in a box).

3. FRET/FLIM acquisitions

NOTE: FRET/FLIM acquisitions in this protocol were performed on a custom-built setup, described in [35] and equipped with a control solution as in [15,17] (**Figure 2**). The setup is now

commercialized by Inscoper and it is made of a spinning-disk microscope with a white laser for pulsed excitation, and a high-rate time-gated intensifier in front of the camera. Temporal gates of 2 ns in a time window of 10 ns are sequentially used to obtain a stack of five time-gated images. These images are then used to calculate the pixel-by-pixel mean fluorescence lifetime according to the following equation: $\tau = \Sigma \Delta t_i \cdot I_i / \Sigma I_i$, where Δt_i corresponds to the delay time of the of the i^{th} gate while I indicates the pixel-by-pixel time-gated intensity image[35,36]. This method ensures rapid FLIM measurements: no fitting or binning steps are required, and lifetime can be calculated in an online mode, with minimal photon budget. The system also presents a user-friendly software interface. However, the same experiment can be performed under any other commercial microscope setup equipped for FLIM measurements.

3.1 To ensure an optimal release of cells from the G2/M block into mitosis, perform experiments at 37 °C. If possible, perform FRET/FLIM experiments with microscope setups equipped with a thermostatic chamber.

3.2 Turn on the thermostatic chamber of the microscope at least 30 min to 1 h before the experiment.

3.3 Switch on the laser, the camera, the microscope setup and the imaging software (**Figure 2**).

3.4 Select the appropriate excitation and emission wavelengths for the donor fluorophore. Convenient wavelengths options are: λ_{ex} 440/10 nm and λ_{em} 483/35 nm for mTurquoise2 (**Figure 3A**); λ_{ex} 488/10 nm and λ_{em} 525/50 nm for GFP) (**Figure 3B**).

3.5 Set the exposure time, generally between 30 and 100 ms (**Figure 3**). Beware that excessive laser power may result in induced phototoxic effects as photobleaching, which could in turn modify the fluorescence lifetime[37]. On the setup, validate the absence of photobleaching events by monitoring the fluorescence intensity of the first gate during time-lapse acquisitions. If variations in the fluorescence intensity are observable, discard the acquisition and adjust laser power.

NOTE: In the setup here, select an exposure time allowing at least 3000 gray levels in the first gate; otherwise the software will not calculate donor lifetime. This gray level value corresponds to the minimal photon budget necessary to obtain relevant lifetime values.

3.6 Before launching FRET/FLIM acquisitions Ensure that cells have entered mitosis, by waiting until the appearance of the bipolar spindle (~20/30 min in U2OS cells). Since mitotic AURKA localizes mainly at this structure, verify mitotic progression by screening the formation of the spindle in cells directly under the microscope, with an external light source (**Figure 1**). Note that the time required for mitotic progression might vary according to the cell line used.

3.7 If treatment with MLN8237 is planned, place the cells under the microscope and allow them to reach metaphase (approx. 20 min after nocodazole washout). Add 250 nM MLN8237

dissolved in DMSO both to cells expressing the donor-only construct and to cells expressing the biosensor.

3.7.1 Control this condition on cells transfected as above and incubate with an equal volume of DMSO. For a better AURKA inhibition, prepare single-use aliquots of MLN8237 in DMSO, store them at -80 °C. Thaw them by placing the aliquots on ice, and discard them after use.

3.7.2 Incubate for 10 min. After this period, the mitotic spindle will shrink and only a single, intense dot is left. A similar phenotype is observed when Lys162Met mutants are used.

3.8 For a better resolution of the mitotic spindle, use at least a 63x objective (**Figure 3**).

3.9 Once found a cell in metaphase (see **Figure 4** as an example of a cell in metaphase), adjust *xyz* coordinates to place it at the center of the field of view.

3.10 For faster images, select one single *z* plane. Choose the plane where the mitotic spindle is more visible or intense.

3.11 Start the recording. The acquisition time may vary according to the FLIM setup used (from few s to min). The majority of the commercial setups available on the market will elaborate both the fluorescence micrograph and the pixel-by-pixel lifetime map. Save both images.

3.12 Acquire at least 10 independent images from each transfection and/or treatment condition.

4. Calculation of ΔLifetime and comparison of FLIM values among donor/acceptor pairs

4.1 Extract lifetime values from the whole pixel-by-pixel lifetime map (i.e., the entire mitotic spindle), or select regions of interest (ROIs) corresponding to specific subregions.

NOTE: According to the FRET/FLIM setup used, lifetime calculations may be performed directly on the acquisition software, or extracted with generic image processing solutions (e.g., Fiji/ImageJ: https://fiji.sc/). Software directly calculating lifetime values (also known as *online mode*) offer a more user-friendly solution, which is suitable for beginners and for microscopy users not fully familiar with FRET/FLIM. On the contrary, the extraction of lifetime values after acquisition often requires a fitting procedure. This option is less accessible to beginners, as some previous knowledge on mathematical models of fitting is necessary.

4.2 Once visualized or extracted, calculate the mean lifetime of the cells expressing the "donor-only" vector (e.g., AURKA-mTurquoise2), hereby *mean donor lifetime*.

4.3 Subtract each independent lifetime value calculated in step 4.1 from the mean donor lifetime. Repeating this step for all cells in all conditions analyzed will give the ΔLifetime for every condition.

4.4 Compare ΔLifetime values for the "donor-only", the "biosensor" and the "K162M", or the DMSO and the MLN8237 conditions.

NOTE: For the "donor-only" condition, ΔLifetime should result in values close to zero and corresponding to the experimental fluctuations of lifetime values. For the "biosensor" condition, ΔLifetime values should yield the net difference between the two constructs (see **Figure 4** for an illustrated example).

4.5 Compare ΔLifetime values among different donor/acceptor pairs.

4.5.1 Compare the "biosensor" conditions: do they show similar ΔLifetime?

4.5.2 Do the "K162M" or the MLN8237 conditions show similar ΔLifetime among them? Is their ΔLifetime similar to the "donor-only" condition?

REPRESENTATIVE RESULTS:

We followed the procedure described above to record the autophosphorylation of AURKA on Thr288 using two biosensors with different spectral properties. We compared the initial GFP-AURKa-mCherry probe[14] with two biosensors with different spectral properties. These two probes rely on the fluorescent donor mTurquoise2 and on a non-fluorescent acceptor (ShadowG) in one case, or a yellow acceptor (superYFP) in a second case. We then inserted the full-length sequence of AURKA within each donor/acceptor pair. To have a negative control for AURKA activation, two strategies can be pursued. First, the use a small ATP-analog (MLN8237) interferes with the binding of ATP in the kinetic pocket of the kinase and prevents its activation[38]. Second, the mutation of Lys162 into Met (K162M), creates a kinase-dead version of each biosensor incapable of activating[14,15,39]. This mutation induces the disruption of a salt bridge normally established between Lys162 and Glu181, which results in a stable opening of the kinetic pocket of the kinase and triggers its overall inactivation[40]. As a negative control for FRET, we used an acceptor-devoid construct (GFP-AURKA or AURKA-mTurquoise2).

After synchronizing cells in G2/M and releasing them into mitosis, we measured the lifetime of all the transfected constructs at the mitotic spindle (**Figure 4**). Of note, this structure was considered as a whole, and no ROIs within the spindle were analyzed. We then calculated ΔLifetime for all conditions. As expected, the lifetime of GFP-AURKA or AURKA-mTurquoise2 (the "donor-only" conditions) was close to 0, indicating that the values measured for these constructs fluctuated around the mean value (**Figure 4A,4B**). Conversely, the ΔLifetime values for GFP-AURKA-mCherry were statistically different from the donor-only condition, with ΔLifetime increasing of ~130 ps (**Figure 4A**). Similar observations were made for shadowG-AURKA-mTurquoise2 and for superYFP-AURKA-mTurquoise2, with ΔLifetime increasing of ~150 and ~220 ps from the donor-only condition, respectively (**Figure 4B,4C**). These data can be easily visualized in single cells with a pseudocolor Lookup Table (LUT). In this case, values of ΔLifetime around 0 are pseudocolored yellow, while more significant differences are pseudocolored red/purple.

Indeed, the pixel-by-pixel LUT was closer to yellow in cells expressing the donor-only constructs, while it was more in the red/purple spectrum in cells expressing either biosensor (**Figure 4A,4B**). This was also observed when the GFP-AURKA-mCherry biosensor was treated with the pharmacological inhibitor MLN8237.

We then analyzed the ΔLifetime of kinase-dead biosensors. These constructs showed intermediate ΔLifetime values: ΔLifetime was significantly higher when compared to the donor-only condition (**Figure 4B,4C**), but it was also significantly lower than their normal counterparts (**Figure 4B,4D**). The comparisons with cells treated with MLN8237 or expressing kinase-dead biosensors are necessary to estimate whether ΔLifetime variations for each donor/acceptor pair are solely linked to the activation of AURKA. In the case of GFP-AURKA-mCherry, ΔLifetime variations are abolished when an AURKA-specific inhibitor is used. Conversely, ΔLifetime variations are mostly, but not exclusively linked to AURKA activation in the case of shadowG-AURKA-mTurquoise2 and of superYFP-AURKA-mTurquoise2.

FIGURE LEGENDS:

Figure 1. GFP (**donor**) **and mCherry** (**acceptor**) **excitation and emission spectra.** Spectra were obtained and adapted from the FP base website (https://www.fpbase.org/), and adjusted to a 480 nm-laser excitation.

Figure 2. Image of the experimental workspace. (1) The control solution; (2) white laser source; (3) CCD camera; (4) microscope setup; (5) external light source/lamp for ocular screening of the sample.

Figure 3. Representative images of the software for FLIM acquisition. (**A, B**) (1) excitation and emission parameters for the donor (CFP in **A**, or GFP in **B**); (2) exposure time; (3) selection of the objective.

Figure 4. Representative images of AURKA FRET biosensors and their negative controls. (**A**) (Micrographs) Fluorescence (green channel) and corresponding pixel-by-pixel ΔLifetime (donor only – biosensor) of U2OS cells expressing GFP-AURKA or GFP-AURKA-mCherry, synchronized at G2/M, released until the bipolar spindle is visible and then treated with DMSO or with MLN8237. ΔLifetime is illustrated with a pseudocolor scale ("Fire" lookup table). (Graph) Corresponding quantification and two-way ANOVA analysis for the indicated conditions. (**B**) (Micrographs) Fluorescence (cyan channel) and corresponding pixel-by-pixel ΔLifetime (donor only – biosensor) of U2OS cells expressing shadowG-AURKA-mTurquoise2 (upper panel) or superYFP-AURKA-mTurquoise2 (lower panel), synchronized at G2/M and released until the bipolar spindle is visible. ΔLifetime is illustrated with a pseudocolor scale ("Fire" lookup table). (Graph) Corresponding quantification and one-way ANOVA analysis of conditions represented in the above micrographs. (**C**) (Micrographs) Images of AURKA-mTurquoise2 (upper panel), shadowG-AURKA K162M-mTurquoise2 (middle panel) and superYFP-AURKA K162M-mTurquoise2 acquired and represented as in the micrographs. (Graph) Two-way ANOVA analysis for the indicated

transfection conditions. The bar in boxplots represents the median; whiskers extend from the min to the max. *n* = 10 cells per condition of one representative experiment (of three). Individual values are represented as dots. Scale bar: 10 µm. **P* < 0.05, ***P* < 0.01, ****P* < 0.001 against each indicated condition in (A) the "AURKA-mTurquoise2" condition in (B), and against each indicated condition in (C). NS: not significant.

DISCUSSION:

Genetically-encoded FRET biosensors are reliable tools to measure the activation of single proteins or of entire signaling pathways[41]. Particularly, the AURKA FRET biosensor constitutes a preferential way to explore the activation of the kinase in time and space. However, some elements deserve special attention when designing or optimizing a FRET biosensor, not only in general terms but more specifically for AURKA.

First, the nature and the relative position of the donor/acceptor FRET pair can be adapted for specific functions of this kinase. AURKA is greatly enriched at the mitotic spindle during mitosis, but it is present throughout the cell cycle and at different subcellular locations (e.g., centrosomes, the nucleus, and mitochondria)[1,2]. If the biosensor is to be used in specific compartments like mitochondria, which can reach acidic pH, the choice of a pH-insensitive donor-acceptor FRET pair as mTurquoise2/shadowG should be made. Moreover, placing the FRET donor at the C-terminus could allow a better visualization of the biosensor at this subcellular compartment, and potentially even optimize FRET detection given that AURKA N-terminus was shown to partially cleave off at mitochondria[16,42].

Second, a yet unexplored way of optimizing the AURKA FRET biosensor would require a more careful design of linkers between full-length AURKA and the donor/acceptor pair. Not only the distance between the fluorescent pair, but also the properties of the linker itself were shown to be key factors to improve FRET efficiency [43–46]. In this light, increasing the rigidity or the flexibility of the linker could either be detrimental to FRET efficiency, or further improve it.

Third, it is known that the overexpression of AURKA induces mitotic spindle abnormalities in a significant proportion of cells[2]. It would be interesting to compare ΔLifetime obtained by expressing the same FRET construct under a strong promoter like cytomegalovirus (CMV) – one of the most common promoters found in mammalian expression vectors – or under the *AURKA* minimal promoter sequence (CTTCCGG)[14,47]. This promoter was previously shown to rescue monopolar or multipolar spindles arising after the knock-down of the kinase, and its use did not induce cell cycle perturbations per se[14,47]. Although FLIM is insensitive to protein expression levels and relative concentrations in the cell[11], benefiting from a thorough comparison of the two promoters on the same biosensor setup would broaden the understanding of the pool of activated AURKA at any given location. In addition, it would provide novel insights on how AURKA activation may change upon overexpression, which is relevant for epithelial and hematologic cancer paradigms.

Last, the downstream FRET application should also be taken into account. A future perspective in the field of AURKA would be to cumulate the kinase conformational biosensor with a substrate-

based biosensor. Analyzing the FRET behavior of two biosensors simultaneously – a process known as multiplex FRET – requires a dark acceptor on the first biosensor to avoid spectral bleed through in the second donor channel. In the context of AURKA, this would open up the exciting new perspective of detecting the activation of the kinase with the first biosensor, and its enzymatic activity towards a given substrate with the second one. Recent developments in multiplexing now allow to cumulate up to three biosensors at a time[48]. Applying a similar method in the context of AURKA could represent a very promising strategy not only to test the activation-activity interplay of the kinase, but also to explore AURKA signaling cascades with unprecedented spatiotemporal resolution.

In conclusion, FRET/FLIM is a convenient way to deepen the knowledge on protein activity. On one hand, it allows to visualize the localization of a given protein in live cells, thanks to at least one fluorescent moiety. On the other hand, it can unravel protein conformational changes, which could be informative on protein activation and/or activity. Therefore, FRET/FLIM and conformational FRET biosensors have the potential of becoming widespread methods to follow signaling pathways in live cells, and with exquisite spatiotemporal resolution.

ACKNOWLEDGMENTS:

We thank the engineers of the Microscopy-Rennes Imaging Center (MRic, BIOSIT, Rennes, France) for advice and help, and particularly X. Pinson for critical reading of the manuscript. MRic is member of the national infrastructure France-BioImaging supported by the French National Research Agency (ANR-10-INBS-04). This work was supported by the *Centre National de la Recherche Scientifique* (CNRS), the *Ligue Contre le Cancer Comités d'Ille et Vilaine, des Côtes d'Armor et du Finistère*, and the *Association pour la Recherche Contre le Cancer (ARC)* to G.B.

DISCLOSURES:

G.B. performed the experiments, wrote and reviewed the manuscript, and provided funding, M.T. reviewed the manuscript and provided support. M.T. is a scientific advisor and shareholder of the Inscoper company (France), which produces the solutions for rapid FLIM measurements shown in this manuscript. Inscoper partially supported the Open Access publication of the manuscript. Inscoper was not involved in experimental design, data handling, nor in the writing of the manuscript.

REFERENCES:

1. Bertolin, G., Tramier, M. Insights into the non-mitotic functions of Aurora kinase A: more than just cell division. *Cellular and Molecular Life Sciences*. (2019).
2. Nikonova, A.S., Astsaturov, I., Serebriiskii, I.G., Dunbrack, R.L., Golemis, E.A. Aurora A kinase (AURKA) in normal and pathological cell division. *Cellular and Molecular Life Sciences*. **70** (4), 661–687 (2013).
3. Walter, A.O., Seghezzi, W., Korver, W., Sheung, J., Lees, E. The mitotic serine/threonine kinase Aurora2/AIK is regulated by phosphorylation and degradation. *Oncogene*. **19** (42), 4906–4916 (2000).
4. Cheetham, G.M.T. Crystal Structure of Aurora-2, an Oncogenic Serine/Threonine Kinase. *Journal of Biological Chemistry*. **277** (45), 42419–42422 (2002).

5. Bayliss, R., Sardon, T., Vernos, I., Conti, E. Structural basis of Aurora-A activation by TPX2 at the mitotic spindle. *Molecular Cell*. **12** (4), 851–862 (2003).
6. Zhang, Y. et al. Identification of the auto-inhibitory domains of Aurora-A kinase. *Biochemical and Biophysical Research Communications*. **357** (2), 347–352 (2007).
7. Littlepage, L.E., Wu, H., Andresson, T., Deanehan, J.K., Amundadottir, L.T., Ruderman, J.V. Identification of phosphorylated residues that affect the activity of the mitotic kinase Aurora-A. *Proceedings of the National Academy of Sciences of the United States of America*. **99** (24), 15440–15445 (2002).
8. Kufer, T.A. et al. Human TPX2 is required for targeting Aurora-A kinase to the spindle. *The Journal of Cell Biology*. **158** (4), 617–623 (2002).
9. Eyers, P.A., Erikson, E., Chen, L.G., Maller, J.L. A novel mechanism for activation of the protein kinase Aurora A. *Current Biology*. **13** (8), 691–697 (2003).
10. Brunet, S. et al. Characterization of the TPX2 Domains Involved in Microtubule Nucleation and Spindle Assembly in Xenopus Egg Extracts. *Molecular Biology of the Cell*. **15** (12), 5318–5328 (2004).
11. Padilla-Parra, S., Tramier, M. FRET microscopy in the living cell: Different approaches, strengths and weaknesses. *BioEssays*. **34** (5), 369–376 (2012).
12. Aoki, K., Kamioka, Y., Matsuda, M. Fluorescence resonance energy transfer imaging of cell signaling from *in vitro* to *in vivo*: Basis of biosensor construction, live imaging, and image processing. *Development, Growth & Differentiation*. **55** (4), 515–522 (2013).
13. Fuller, B.G. et al. Midzone activation of aurora B in anaphase produces an intracellular phosphorylation gradient. *Nature*. **453** (7198), 1132–1136 (2008).
14. Bertolin, G. et al. A FRET biosensor reveals spatiotemporal activation and functions of aurora kinase A in living cells. *Nature Communications*. **7**, 12674 (2016).
15. Bertolin, G. et al. Optimized FRET Pairs and Quantification Approaches To Detect the Activation of Aurora Kinase A at Mitosis. *ACS Sensors*. **4** (8), 2018–2027 (2019).
16. Bertolin, G. et al. Aurora kinase A localises to mitochondria to control organelle dynamics and energy production. *eLife*. **7** (2018).
17. Sizaire, F., Le Marchand, G., Pécréaux, J., Bouchareb, O., Tramier, M. Automated screening of AURKA activity based on a genetically encoded FRET biosensor using fluorescence lifetime imaging microscopy. *Methods and Applications in Fluorescence*. **8** (2), 024006 (2020).
18. Demeautis, C. et al. Multiplexing PKA and ERK1&2 kinases FRET biosensors in living cells using single excitation wavelength dual colour FLIM. *Scientific Reports*. **7**, 41026 (2017).
19. Ringer, P. et al. Multiplexing molecular tension sensors reveals piconewton force gradient across talin-1. *Nature Methods*. **14** (11), 1090–1096 (2017).
20. Nagai, T., Yamada, S., Tominaga, T., Ichikawa, M., Miyawaki, A. Expanded dynamic range of fluorescent indicators for Ca(2+) by circularly permuted yellow fluorescent proteins. *Proceedings of the National Academy of Sciences of the United States of America*. **101** (29), 10554–10559 (2004).
21. Klarenbeek, J., Goedhart, J., Batenburg, A. van, Groenewald, D., Jalink, K. Fourth-Generation Epac-Based FRET Sensors for cAMP Feature Exceptional Brightness, Photostability and Dynamic Range: Characterization of Dedicated Sensors for FLIM, for Ratiometry and with High Affinity. *PLOS ONE*. **10** (4), e0122513 (2015).
22. Fritz, R.D. et al. A Versatile Toolkit to Produce Sensitive FRET Biosensors to Visualize

Signaling in Time and Space. *Science Signaling*. **6** (285), rs12–rs12 (2013).
23. Mastop, M. et al. Characterization of a spectrally diverse set of fluorescent proteins as FRET acceptors for mTurquoise2. *Scientific Reports*. **7** (1), 11999 (2017).
24. van der Krogt, G.N.M., Ogink, J., Ponsioen, B., Jalink, K. A Comparison of Donor-Acceptor Pairs for Genetically Encoded FRET Sensors: Application to the Epac cAMP Sensor as an Example. *PLoS ONE*. **3** (4), e1916 (2008).
25. Cranfill, P.J. et al. Quantitative assessment of fluorescent proteins. *Nature Methods*. **13** (7), 557–562 (2016).
26. Goedhart, J. et al. Structure-guided evolution of cyan fluorescent proteins towards a quantum yield of 93%. *Nature Communications*. **3** (1) (2012).
27. Mérola, F. et al. Newly engineered cyan fluorescent proteins with enhanced performances for live cell FRET imaging. *Biotechnology Journal*. **9** (2), 180–191 (2014).
28. Erard, M. et al. Minimum set of mutations needed to optimize cyan fluorescent proteins for live cell imaging. *Molecular BioSystems*. **9** (2), 258–267 (2013).
29. Tramier, M., Zahid, M., Mevel, J.-C., Masse, M.-J., Coppey-Moisan, M. Sensitivity of CFP/YFP and GFP/mCherry pairs to donor photobleaching on FRET determination by fluorescence lifetime imaging microscopy in living cells. *Microscopy Research and Technique*. **69** (11), 933–939 (2006).
30. Padilla-Parra, S. et al. Quantitative Comparison of Different Fluorescent Protein Couples for Fast FRET-FLIM Acquisition. *Biophysical Journal*. **97** (8), 2368–2376 (2009).
31. Burgstaller, S. et al. pH-Lemon, a Fluorescent Protein-Based pH Reporter for Acidic Compartments. *ACS Sensors*. (2019).
32. Bindels, D.S. et al. mScarlet: a bright monomeric red fluorescent protein for cellular imaging. *Nature Methods*. **14** (1), 53–56 (2016).
33. Murakoshi, H., Shibata, A.C.E., Nakahata, Y., Nabekura, J. A dark green fluorescent protein as an acceptor for measurement of Förster resonance energy transfer. *Scientific Reports*. **5**, 15334 (2015).
34. Murakoshi, H., Shibata, A.C.E. ShadowY: a dark yellow fluorescent protein for FLIM-based FRET measurement. *Scientific Reports*. **7** (1), 6791 (2017).
35. Leray, A., Padilla-Parra, S., Roul, J., Héliot, L., Tramier, M. Spatio-Temporal Quantification of FRET in living cells by fast time-domain FLIM: a comparative study of non-fitting methods [corrected]. *PloS One*. **8** (7), e69335 (2013).
36. Padilla-Parra, S., Audugé, N., Coppey-Moisan, M., Tramier, M. Quantitative FRET analysis by fast acquisition time domain FLIM at high spatial resolution in living cells. *Biophysical Journal*. **95** (6), 2976–2988 (2008).
37. Song, L., Hennink, E.J., Young, I.T., Tanke, H.J. Photobleaching kinetics of fluorescein in quantitative fluorescence microscopy. *Biophysical Journal*. **68** (6), 2588–2600 (1995).
38. Manfredi, M.G. et al. Characterization of Alisertib (MLN8237), an investigational small-molecule inhibitor of aurora A kinase using novel in vivo pharmacodynamic assays. *Clinical Cancer Research: An Official Journal of the American Association for Cancer Research*. **17** (24), 7614–7624 (2011).
39. Katayama, H. et al. Phosphorylation by aurora kinase A induces Mdm2-mediated destabilization and inhibition of p53. *Nature Genetics*. **36** (1), 55–62 (2004).
40. Nowakowski, J. et al. Structures of the Cancer-Related Aurora-A, FAK, and EphA2 Protein

Kinases from Nanovolume Crystallography. *Structure*. **10** (12), 1659–1667 (2002).
41. Palmer, A.E., Qin, Y., Park, J.G., McCombs, J.E. Design and application of genetically encoded biosensors. *Trends in Biotechnology*. **29** (3), 144–152 (2011).
42. Grant, R. et al. Constitutive regulation of mitochondrial morphology by Aurora A kinase depends on a predicted cryptic targeting sequence at the N-terminus. *Open Biology*. **8** (6), 170272 (2018).
43. Shimozono, S., Miyawaki, A. Engineering FRET Constructs Using CFP and YFP. *Methods in Cell Biology*. **85**, 381–393 (2008).
44. Komatsu, N. et al. Development of an optimized backbone of FRET biosensors for kinases and GTPases. *Molecular Biology of the Cell*. **22** (23), 4647–4656 (2011).
45. Schifferer, M., Griesbeck, O. A Dynamic FRET Reporter of Gene Expression Improved by Functional Screening. *Journal of the American Chemical Society*. **134** (37), 15185–15188 (2012).
46. Peroza, E.A., Boumezbeur, A.-H., Zamboni, N. Rapid, randomized development of genetically encoded FRET sensors for small molecules. *Analyst*. **140** (13), 4540–4548 (2015).
47. Reboutier, D. et al. Aurora A is involved in central spindle assembly through phosphorylation of Ser 19 in P150Glued. *The Journal of Cell Biology*. **201** (1), 65–79 (2013).
48. Mo, G.C.H., Posner, C., Rodriguez, E.A., Sun, T., Zhang, J. A rationally enhanced red fluorescent protein expands the utility of FRET biosensors. *Nature Communications*. **11** (1), 1848 (2020).

Figure 1 in .png format

Click here to access/download;Figure;Fig. 1.png

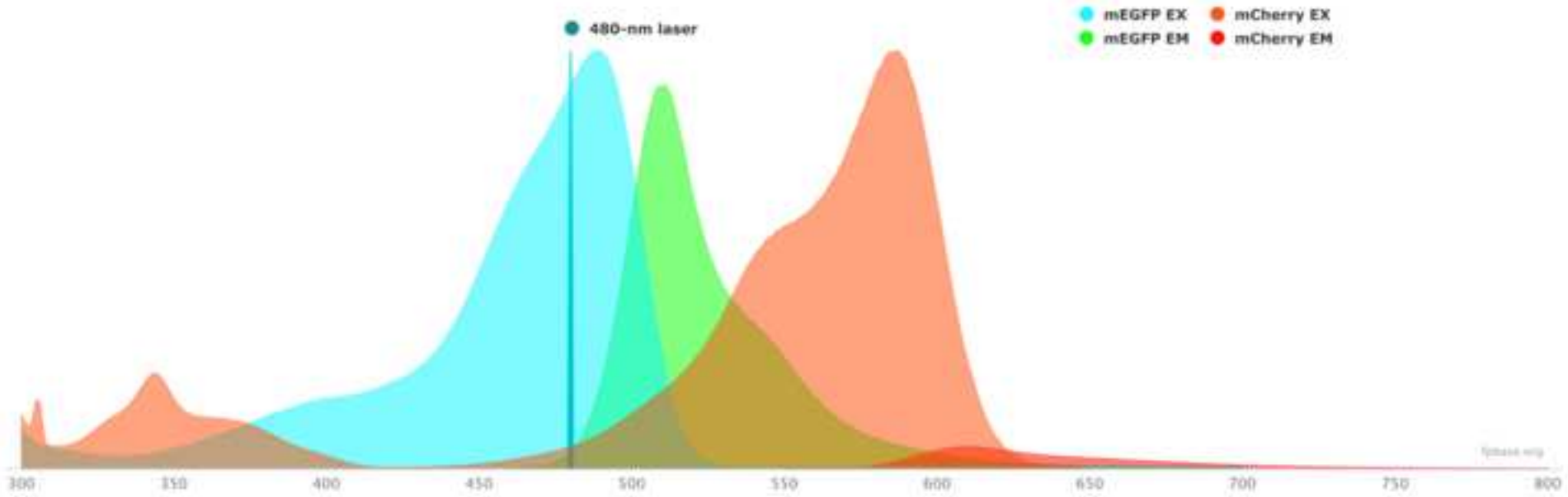

Figure 2 in .png format

Click here to access/download;Figure;Fig. 2.png

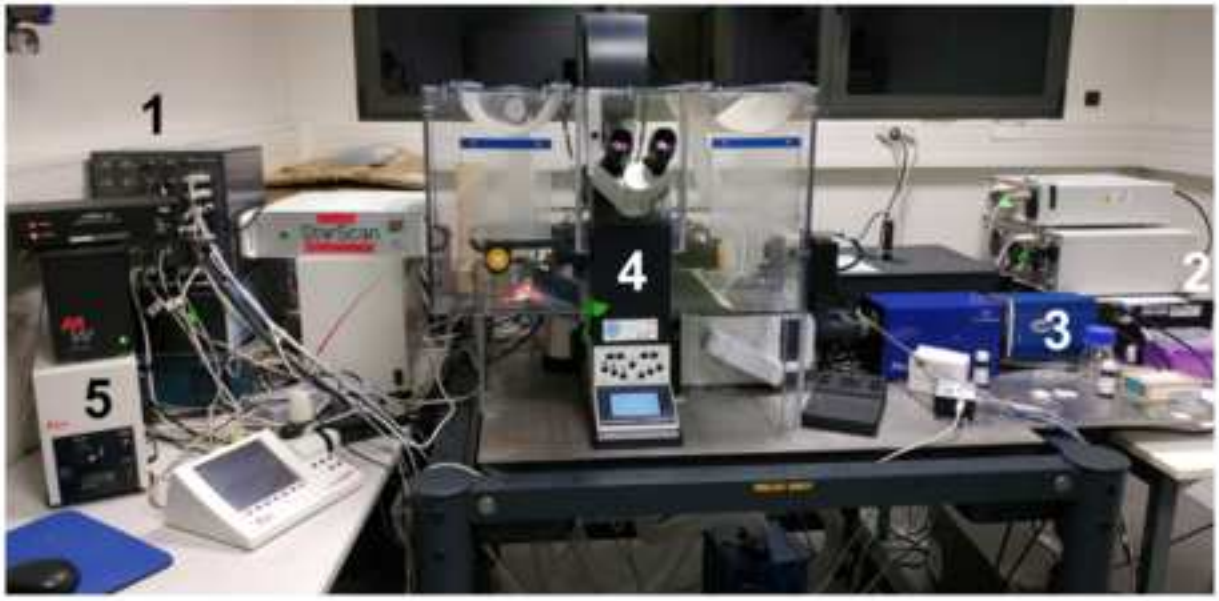

Figure 3 in .png format

Click here to access/download;Figure;Fig. 3.png

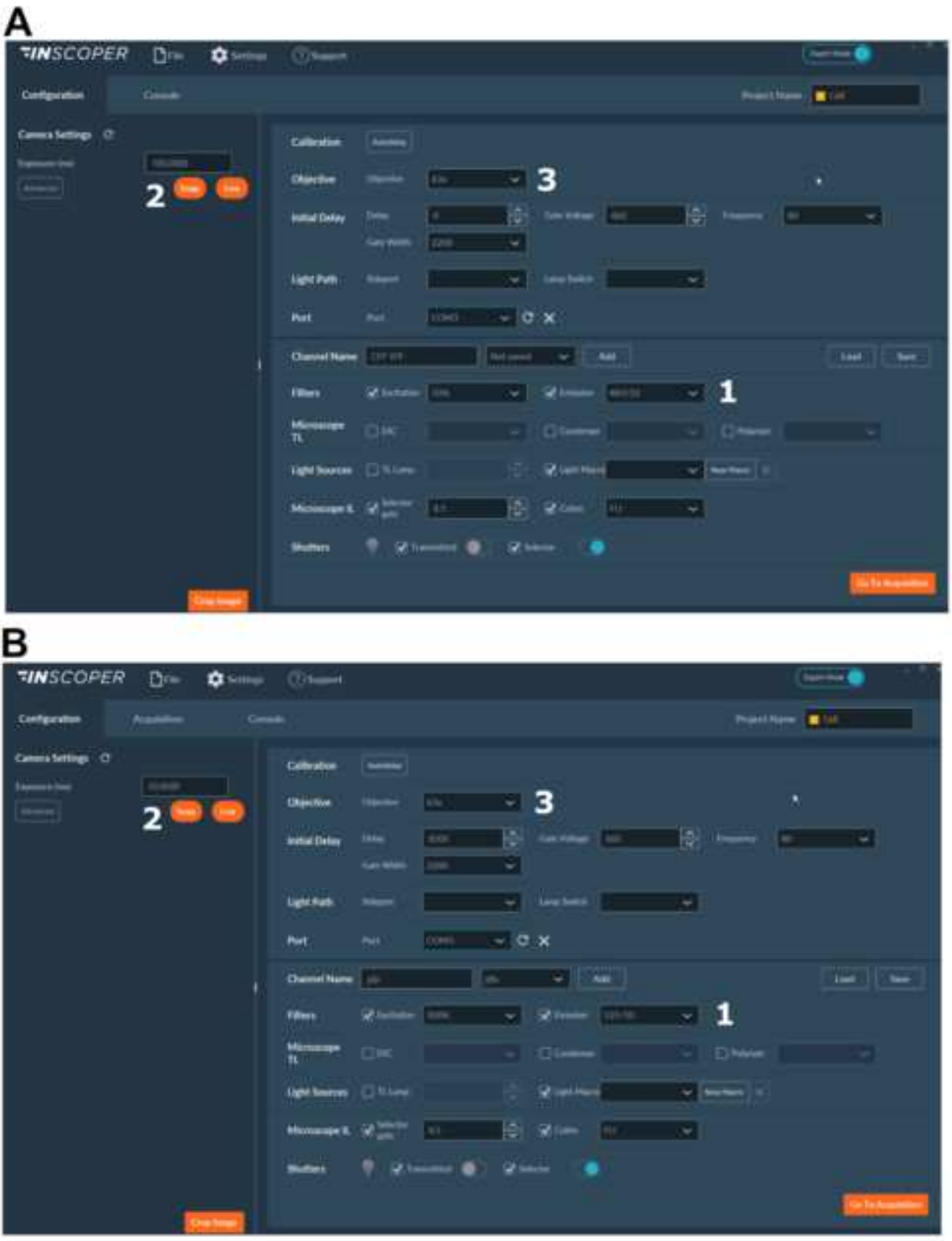

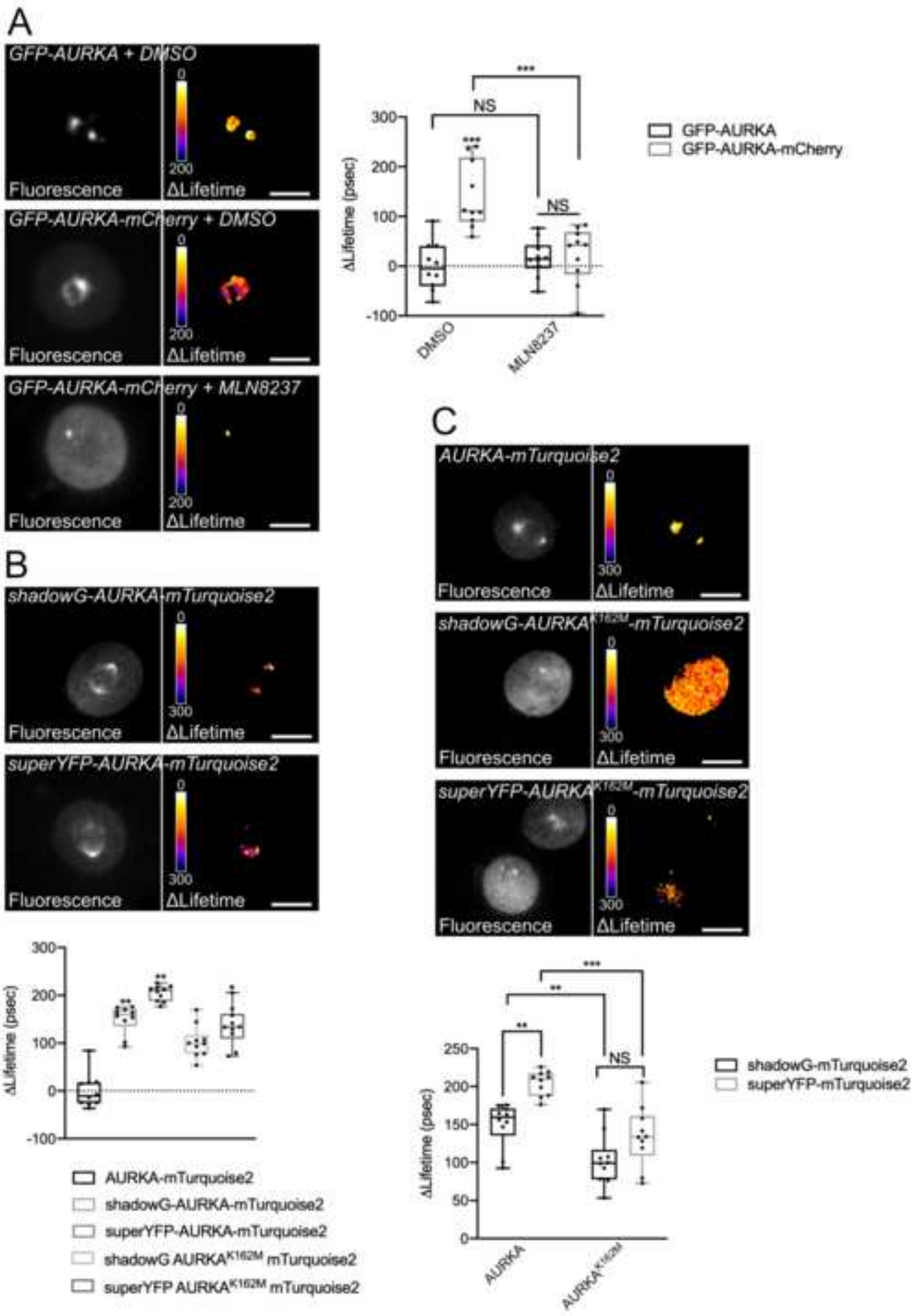

Figure 1 in .svg format as requested by JoVE

Click here to access/download

Video or Animated Figure

Fig. 1.svg

Figure 2 in .svg format as requested by JoVE

Click here to access/download

Video or Animated Figure

Fig. 2.svg

Figure 3 in .svg format as requested by JoVE

Figure 4 in .svg format as requested by JoVE

Table of Materials

Click here to access/download;Table of Materials;JoVE_Materials_Bertolin et al_Revised.xls

Name of Material/ Equipment	Brand	Distributor	Catalog Number
Alisertib (MLN8237)		SelleckChem	S1133
Dulbecco's Modified Eagle Medium (DMEM)	Gibco	ThermoFischer Scientific	41966052
Fetal Bovine Serum (FBS)	Gibco	ThermoFischer Scientific	10270106
L15	Gibco	ThermoFischer Scientific	21083027
LabTek		Nunc	2515380
Nocodazole	Sigma-Aldrich	Merck	M1404
Penicillin/Streptomycin	Gibco	ThermoFischer Scientific	15140122
Phosphate Buffer Saline (PBS)	Gibco	ThermoFischer Scientific	14190169
Trypsin/EDTA	Gibco	ThermoFischer Scientific	25300096

Comments/Description
Use at a 250 nM final dilution
High glucose + L-glutamine + Sodium pyruvate
Leibovitz's L15 medium + L-glutamine, no Phenol red
Use at a 100 ng/mL final dilution
Penicillin-Streptomycin 10,000 U/mL (100x)
DPBS, no calcium, no magnesium
Trypsin-EDTA 0.05%, Phenol Red (1x)

Editorial Comments:

• *Please take this opportunity to thoroughly proofread the manuscript to ensure that there are no spelling or grammatical errors.*

We corrected the spelling and grammar errors still present in the manuscript.

• *Protocol Language: Please ensure that ALL text in the protocol section is written in the imperative voice/tense as if you are telling someone how to do the technique (i.e. "Do this", "Measure that" etc.) Any text that cannot be written in the imperative tense may be added as a "Note", however, notes should be used sparingly and actions should be described in the imperative tense wherever possible. Examples NOT in the imperative: 1.3,-1.4.3*

We ensured that all text protocol is in the imperative form.

• *Protocol Detail: Please note that your protocol will be used to generate the script for the video, and must contain everything that you would like shown in the video. Please ensure that all specific details (e.g. button clicks for software actions, numerical values for settings, etc) have been added to your protocol steps. There should be enough detail in each step to supplement the actions seen in the video so that viewers can easily replicate the protocol. Please limit protocol length to 10 pages.*

The protocol is limited to 10 pages.

• *Protocol Numbering: All steps should be lined up at the left margin with no indentations. There must also be a one-line space between each protocol step.*

The protocol has been revised accordingly.

• *Protocol Highlight: After you have made all of the recommended changes to your protocol (listed above), please re-evaluate the length of your protocol section. There is a 10-page limit for the protocol text, and a 3- page limit for filmable content. If your protocol is longer than 3 pages, please highlight ~2.5 pages or less of text (which includes headings and spaces) in yellow, to identify which steps should be visualized to tell the most cohesive story of your protocol steps.*
1) The highlighting must include all relevant details that are required to perform the step. For example, if step 2.5 is highlighted for filming and the details of how to perform the step are given in steps 2.5.1 and 2.5.2, then the sub-steps where the details are provided must be included in the highlighting.
2) The highlighted steps should form a cohesive narrative, that is, there must be a logical flow from one highlighted step to the next.
3) Please highlight complete sentences (not parts of sentences). Include sub-headings and spaces when calculating the final highlighted length.
4) Notes cannot be filmed and should be excluded from highlighting.
5) Please bear in mind that software steps without a graphical user interface/calculations/ command line scripting cannot be filmed.

The protocol has been revised accordingly.

• *Discussion: JoVE articles are focused on the methods and the protocol, thus the discussion should be similarly focused. Please ensure that the discussion covers the following in detail and in paragraph form*

(3-6 paragraphs): 1) modifications and troubleshooting, 2) limitations of the technique, 3) significance with respect to existing methods, 4) future applications and 5) critical steps within the protocol.

We made sure that the discussion follows this structure

• *If your figures and tables are original and not published previously or you have already obtained figure permissions, please ignore this comment. If you are re-using figures from a previous publication, you must obtain explicit permission to re-use the figure from the previous publisher (this can be in the form of a letter from an editor or a link to the editorial policies that allows you to re-publish the figure). Please upload the text of the re-print permission (may be copied and pasted from an email/website) as a Word document to the Editorial Manager site in the "Supplemental files (as requested by JoVE)" section. Please also cite the figure appropriately in the figure legend, i.e. "This figure has been modified from [citation]."*

Figures and tables of the present manuscript are original.

Reviewer #1:

Manuscript Summary:

Overall, the protocol is succinct and largely useful to understand FLIM FRET. Sufficient background is given to understand the scope of the protocol. However, key pieces of information are missing from the protocol that would allow it to practically benefit a wider community.

We thank reviewer #1 for taking the time to review our manuscript, for providing generous feedback and for understanding the usefulness of our protocol for the FRET/FLIM community.

Major Concerns:

1. Even though the AURKA FRET biosensor has been tested before, in 1.3 or other appropriate sections, please either describe only the use of the demonstrated FRET pairs, or inform readers that FRET biosensor activity increases or decreases depending on both distance and orientation changes and hence the choice of the FRET pair.

We see the reviewer's point on this particular aspect. To homogenise this protocol with the previous versions of our biosensors, we replaced the mTurquoise2/mNeonGreen pair with the mEGFP/mCherry one in **Figure 1 of the revised version of the manuscript**. This corresponds to our first version of our biosensor (see Bertolin et al, *Nat Comm*. 2016). Accordingly, we amended the protocol to account for this change (**Lines 163, 166, 172, 178, and Results section**). To help the reader to familiarize with this first version of the AURKA biosensor, we modified **Fig. 4** and we added representative pictures and the corresponding ΔLifetime quantification of GFP-AURKA and of GFP-AURKA-mCherry in panel A. In the same panel, we also show the behavior of the biosensor upon treatment with MLN8237. In the manuscript, we also take advantage of these new pictures and their corresponding quantifications to further underline how the AURKA biosensor must be controlled (see point 2 of the present **Response**). We hope that the reviewer will be satisfied with these changes.

2. Donor only control is insufficient. Static, kinase-dead or chemical inhibition control is necessary to establish the validity of each FRET pair. While this is performed in Fig. 4, this experimental design should be clearly rationalized and emphasized.

We agree with the reviewer that a kinase-dead construct and/or AURKA inhibitors as MLN8237 are required to validate each (new) version of the AURKA biosensor. Although the need for these controls is already mentioned in the original version of the manuscript (**point 2.5.1**), we agree on the fact that the rationale of such controls should be made clearer to the readers. In light of the reviewer's comment, we emphasized this point in the revised version of the manuscript (**Lines 221-226**). We now describe the use of MLN8237 more thoroughly in the manuscript (**Lines 319-327; 385-390**), and we added representative pictures and quantifications of DMSO versus MLN8237-treated cells in the **revised Fig.4A**. We hope that the reviewer will deem these new elements sufficient.

3. Cell cycle synchronization efficiency must be high to retain statistical significance in subsequent quantitation. Thus in 2.6, please detail what observations would help identify issues in synchronization efficiency.

We agree with the reviewer that synchronisation efficiency is a significant parameter to monitor, as it can vary among cell types. Following his/her comment, we now suggest the reader to verify this parameter using flow cytometry approaches prior to FRET/FLIM analyses (**Lines 246-250**).

4. In 2.7.3, please indicate whether pH indicators in the medium will affect FLIM imaging results.

We thank the reviewer for bringing this point to our attention! We agree that it is very important to state in the manuscript that substances in the cell medium as pH indicators and serum components as riboflavin could affect lifetime values, as they are a source of autofluorescence. Therefore, it is preferable to use imaging media that lack additives as phenol red or specific components to eliminate potential sources of unwanted fluorescence that could perturb FLIM values. These considerations are now present in the revised version of the manuscript (**Lines 262-264**).

5. The purpose of this article is to permit reliable FLIM AURKA biosensing on many platforms. While figures of a proprietary interface is helpful, it is not available to all. The use of ImageJ/Fiji macros without basic understanding should also not be encouraged. Please make every effort to describe the algorithms behind the software (binning, common fitting methods, etc) so readers can assess and perform calculations properly.

We thank the reviewer for his/her suggestion, and for helping us to broaden the impact of our FLIM calculation setup and method. A more detailed explanation is now available in the revised version of the manuscript, **lines 281-288**. In brief, the "is made of a spinning-disk microscope with a white laser for pulsed excitation, and a high-rate time-gated intensifier in front of the camera. Temporal gates of 2 nsec in a time window of 10 nsec are sequentially used to obtain a stack of five time-gated images. These images are then used to calculate the pixel-by-pixel mean fluorescence lifetime according to the following equation: $\tau = \Sigma\Delta t_i \cdot I_i / \Sigma I_i$, where Δt_i corresponds to the delay time of the of the i^{th} gate while *I* indicates the pixel-by-pixel time-gated intensity image. This method ensures rapid FLIM measurements: no fitting or binning steps are required, and lifetime can be calculated in an online mode, with minimal photon budget". We also added two additional references in the manuscript for a more detailed understating of our method.

6. In 3.4, the brief mentioning of exposure time is insufficient, as it does not consider other microscope set up regarding gain, camera sensitivity, or other settings. Please revise. Please add observations and

methods to identify characteristic photobleaching time scale to avoid unintended effects in FLIM datasets.

We agree with the reviewer that users should be able to detect photobleaching events potentially affecting FLIM datasets. On the Inscoper setup, the user needs to monitor the fluorescence intensity of five images issued from the first gate. If no variations are observed/calculated, the user can autonomously assess the absence of photobleaching during the acquisition. This is now available in the revised version of the manuscript, **lines 301-306**.

7. Fig. 4 C/D are redundant. Please either add control to D, or add statistical significance to C.

We thank the reviewer for his/her considerations. We believe that the two graphs deliver a different message. On one hand, C is needed to appreciate the differences between a donor-only construct and biosensors, and statistical significance is present to help the reader on data interpretation. On the other hand, D is needed to appreciate the differences between normal and kinase-dead biosensors carrying two different donor/acceptor pairs. Following up on the reviewers' comments concerning the importance of different types of controls to validate any new AURKA biosensor (see **point 2 of the present response and lines 221-226 of the revised version of the manuscript**), we believe that both graphs are needed to better illustrate what parameters the end-user should take into account. Of note, the C/D panels of the revised Fig. 4 are now fused to panels B and C, respectively.

8. In 4.5, the authors should address the additional considerations directly relevant to AURKA instead of posing open-ended questions.

Following up on the previous comment and on data presented in Fig. 4, we believe that our open-ended questions allow users to perform a "checklist" with the key parameters needed to interpret the behaviour of the AURKA biosensor(s) in their hands. Such checklist aims at assessing the efficiency of new variants of the AURKA biosensor, or to confirm that of the existing ones. Therefore, we believe that these considerations are important in a protocol manuscript as those published by *JoVE*. To further underline the importance of this point for us, we removed the "*If pertinent*" formulation at the beginning of paragraph 4.5 (**Line 370**).

9. The authors describe multiplexing FRET biosensors as a challenging (P.9-10), which is inaccurate. There are published methods to multiplex 3 or more FRET biosensors. The authors should cite additional references to directly reflect the current state of development and suggest ways that the current protocol can interact with these works.

Again, we thank the reviewer for bringing this specific point to our attention! We agree on the fact that robust techniques exist for multiplexing FRET biosensors, and that multiplex approaches start to be used by an increasing number of teams. In these terms, we agree that "*challenging*" is an inappropriate word, and we modified it in the revised version of the manuscript with "*A future perspective in the field of AURKA*" (**lines 491-492**). We also added some perspective to the use of 3 biosensors for multiplexing AURKA functions (**lines 497-501**), as well as an additional reference.

10. The authors should describe biological drawbacks and limitations of the approach, especially in terms of the over-expression of a key, active kinase.

We thank the reviewer for his/her comment. We agree on the fact that caution should be exercised when massively overexpressing the AURKA biosensor. Considerations on the pertinence and/or limitation of a massive overexpression versus a physiological-like expression of the AURKA biosensor are present in **lines 478-489** of the manuscript. We hope that these elements will be deemed sufficient by the reviewer.

Minor Concerns:
1. Please remove the typo: - which can reach acidic pH - ","; p. 9.

We thank the reviewer for detecting this typo, which has been removed in the revised version of the manuscript (**line 466**).

Reviewer #2:
Manuscript Summary:
Bertolin el al. studied the AURKA a multifunctional protein in the cell cycle. Its overexpression plays the important role in cancer. They have created a FRET based tool to study the activation and inactivation process of AURKA. The work is well planned and the fluorescence technology along with fluorescent probes became efficient way to study physiology activities. This paper reported fluorescent probe and it can be accepted after minor revision:

We thank Reviewer #2 for taking the time to evaluate our manuscript, and for his/her encouraging and positive comments concerning the structure of the manuscript and the efficiency of our method.

Minor Concerns:
1. At page no. 2-3, strategy of choosing the donor/acceptor pair details is useless. Just give in brief.
2. At page no 3, verifying of spectral properties of FRET is in excess. Shorten it.
3. At page no 5-6 FRET-FLIM protocol is too much. Give briefly only.

We thank the reviewer for providing suggestions on how to improve the flow of our manuscript. We agree that experimented users could find the choice strategy for donor/acceptor pairs, spectral properties of fluorophores and an in-depth FRET/FLIM protocol somehow excessive. However, we believe that readers with a low experience in FRET/FLIM analyses would benefit from a more thorough description of these key parameters. We also believe that these considerations are important in a protocol manuscript as those published by *JoVE*, which aims at providing step-by-step instructions on how to perform cutting-edge experiments and how to make them available to a larger community.

4. All figures are very indistinct. Repeat them or depict clearly to get it easy for readers.

We are sorry that figure rendering was of poor quality. We believe that this is due to the PDF conversion at the submission step. We will make sure that the final figures do not show a loss in resolution.

Reviewer #3:
Manuscript Summary:
In this paper, Bertolin and colleagues set out to develop a novel AURKA FRET biosensor that detects the alteration of protein conformation change by Thr288 autophosphorylation. This FRET biosensor

consists of a donner fluorescent protein, an acceptor fluorescent protein, and full-length Aurora kinase A protein. The authors quantified this kinase activity by Fluorescence Lifetime Imaging Microscopy with synchronized U2OS cells under different combinations of fluorescent proteins and kinase-dead mutant. The authors also provided a step-by-step protocol for the design of FRET biosensor and the analysis of Fluorescence Lifetime Imaging Microscopy results.

We thank Reviewer #3 for taking the time to evaluate our manuscript and for providing constructive comments.

Major Concerns:
1. During the activation of AURKA, two-step conformation change has been revealed by structural studies. Is this biosensor able to detect the two-step activation? The authors needed to mention the sensitivity of this biosensor and how much improved from the substate-based biosensor.

We thank the reviewer for this very interesting consideration. It is true that AURKA is known to be activated in a two-step process, which is driven by the AURKA partner TPX2 at mitosis. However, structural data also indicated that AURKA can be activated at the same extent with and without TPX2, meaning that autophosphorylation on Thr288 is sufficient to fully "prime" the kinase for activation (Zorba et al, *eLife* 2014). We never tried to assess whether the biosensor could also report on the second conformational change induced by TPX2. Therefore, we are unable to comment on its sensitivity concerning the two steps.

In addition, a substrate-based FRET biosensor has been used to detect the activity of AURKB at mitosis (Fuller et al, *Nature* 2008). Since it relies on a generic consensus sequence shared both by AURKA and AURKB, it can be considered a general reporter of the activity of the AURK family. These two biosensors are not mutually exclusive, but rather detect two distinct events which we find hard to compare: the conformational biosensor detects the activation/priming of AURKA, while the substrate-based one detects its enzymatic activity. We believe that these considerations go beyond the scope of the present protocol.

2. This FRET sensor uses the full-length of Aurora kinase A protein. Is full-length protein required to detect the conformational change? I concerned that the expression of a full-length protein with fluorescent proteins mimics the overexpression of Aurora kinase A protein and interferes with the endogenous cell cycle mechanism.

We agree with the reviewer on his/her concern. Indeed, one of the key parameters in the validation strategy of the AURKA biosensor focused on demonstrating that the biosensor could functionally replace the endogenous protein, and that its response was not interfering with the cell cycle. Indeed, the expression of full-length AURKA under its endogenous promoter rescued mitotic spindle abnormalities, and no cell cycle perturbation was observed (Bertolin et al, *Nat Comm,* 2016). We further comment on this aspect in **lines 482-484** of the present manuscript.

3. For negative control experiments, has non-phosphorylatable mutant been tested such as T288A? K162M also inhibits the conformation change of target protein (Fig 4), but it was not clear to me the relationships of the autophosphorylation of T288 and K162 from the manuscript.

We thank the reviewer for his/her comment. Although Thr288 is the key residue being phosphorylated in the process of AURKA activation, its mutation into Ala would trigger the phosphorylation of Thr287. With this nearby residue modified, AURKA is activated to the same extent as when Thr288 is

phosphorylated. Therefore, a Thr288Ala mutant would not abolish AURKA activation. On the contrary, a Lys162Met mutation induces the disruption of a salt bridge normally established between Lys162 and Glu181, which results in a stable opening of the kinetic pocket of the kinase and which triggers its overall inactivation (Nowakowski et al, *Structure* 2002). This point has been partially introduced in the Results section (**Lines 385-390**).

Minor Concerns:
Figure 1
1. What is the Y-axis?

These spectra are issued from the FP base website, where the Y axis is the intensity normalised to 1.

2. Why is the peak of mNeonGreen EM lower than others?

The peak of mNeonGreen is lower than the others because the fluorophore emission is extremely low with a 440-nm laser. This is the same for mCherry in the new **Fig. 1** of the revised version of the manuscript. As the donor lifetime is the only key parameter in FRET/FLIM analyses, the wavelength used to measure it must be optimal for this fluorescent moiety. Its suitability for the emission of the acceptor is not mandatory.

Protocol 1.3.2
1. mNeon2 → mNeonGreen?

We thank the reviewer for detecting this typo, which has now been corrected.

Figure 4A, 4B
1. "After synchronizing cells in G2/M and releasing them into mitosis, we measured the lifetime of all the transfected constructs at the mitotic spindle (Figure 4). Of note, this structure was considered as a whole, and no ROIs within the spindle were analyzed."
What kind of criteria (image processing thresholding) did the authors use to plot ΔLifetime? It looks the only bright area was used to measure ΔLifetime.

We thank the reviewer for this important point. The Inscoper solution allows to calculate donor lifetime values only if the fluorescence intensity of the first gate is above 3000 gray levels (**lines 307-310** of the revised version of the manuscript). This imaging parameter often takes into account both the spindle and the cytosol, and this is particularly true for the K162M mutant which shows a more intense fluorescence in the cytosol (see comment below for further details). As stated in the manuscript, the user can (i) analyse lifetime values on the entire cell and regardless of the subcellular localisation of AURKA, or (ii) draw ROIs on selected areas. In the case of the mitotic spindle, we drew a ROI on the entire mitotic spindle and we extracted its lifetime values.

2. In Fig 4B middle and bottom panel, the FRET sensor is distributed almost evenly in the cell. Does bipolar spindle form correctly inside the cell or K162M mutant lost the binding ability to the spindle?

We agree with the reviewer that the K162M mutant has a different subcellular distribution compared to the normal protein. In the case of AURKA, the expression of this mutation induces monopolar or multipolar mitotic spindles, which are incapable of performing a correct cell division. In either case, the

kinase does not localize correctly to this structure, and it is found to be more abundant in the cytosol. A similar phenotype is retrieved upon treatment with MLN8237. We agree with the reviewer that this is an important element to point out, and we now detail this feature in the protocol as a piece of information to the end-user in terms of treatment efficacy or of transfection efficiency (**Lines 325-327**).

jove JOURNAL OF VISUALIZED EXPERIMENTS
1 Alewife Center #200
Cambridge, MA 02140
tel. 617.945.9051
www.jove.com

ARTICLE AND VIDEO LICENSE AGREEMENT

Title of Article:	Real-time monitoring of Aurora kinase A activation using conformational FRET biosensors in live cells
Author(s):	Giulia Bertolin, Gilles Le Marchand, Marc Tramier

Item 1: The Author elects to have the Materials be made available (as described at http://www.jove.com/publish) via:

☐ Standard Access ☑ Open Access

Item 2: Please select one of the following items:

☑ The Author is **NOT** a United States government employee.

☐ The Author is a United States government employee and the Materials were prepared in the course of his or her duties as a United States government employee.

ARTICLE AND VIDEO LICENSE AGREEMENT

1. **Defined Terms.** As used in this Article and Video License Agreement, the following terms shall have the following meanings: "**Agreement**" means this Article and Video License Agreement; "**Article**" means the article specified on the last page of this Agreement, including any associated materials such as texts, figures, tables, artwork, abstracts, or summaries contained therein; "**Author**" means the author who is a signatory to this Agreement; "**Collective Work**" means a work, such as a periodical issue, anthology or encyclopedia, in which the Materials in their entirety in unmodified form, along with a number of other contributions, constituting separate and independent works in themselves, are assembled into a collective whole; "**CRC License**" means the Creative Commons Attribution-Non Commercial-No Derivs 3.0 Unported Agreement, the terms and conditions of which can be found at: http://creativecommons.org/licenses/by-nc-nd/3.0/legalcode; "**Derivative Work**" means a work based upon the Materials or upon the Materials and other pre-existing works, such as a translation, musical arrangement, dramatization, fictionalization, motion picture version, sound recording, art reproduction, abridgment, condensation, or any other form in which the Materials may be recast, transformed, or adapted; "**Institution**" means the institution, listed on the last page of this Agreement, by which the Author was employed at the time of the creation of the Materials; "**JoVE**" means MyJove Corporation, a Massachusetts corporation and the publisher of The Journal of Visualized Experiments; "**Materials**" means the Article and / or the Video; "**Parties**" means the Author and JoVE; "**Video**" means any video(s) made by the Author, alone or in conjunction with any other parties, or by JoVE or its affiliates or agents, individually or in collaboration with the Author or any other parties, incorporating all or any portion of the Article, and in which the Author may or may not appear.

2. **Background.** The Author, who is the author of the Article, in order to ensure the dissemination and protection of the Article, desires to have the JoVE publish the Article and create and transmit videos based on the Article. In furtherance of such goals, the Parties desire to memorialize in this Agreement the respective rights of each Party in and to the Article and the Video.

3. **Grant of Rights in Article.** In consideration of JoVE agreeing to publish the Article, the Author hereby grants to JoVE, subject to **Sections 4** and **7** below, the exclusive, royalty-free, perpetual (for the full term of copyright in the Article, including any extensions thereto) license (a) to publish, reproduce, distribute, display and store the Article in all forms, formats and media whether now known or hereafter developed (including without limitation in print, digital and electronic form) throughout the world, (b) to translate the Article into other languages, create adaptations, summaries or extracts of the Article or other Derivative Works (including, without limitation, the Video) or Collective Works based on all or any portion of the Article and exercise all of the rights set forth in (a) above in such translations, adaptations, summaries, extracts, Derivative Works or Collective Works and(c) to license others to do any or all of the above. The foregoing rights may be exercised in all media and formats, whether now known or hereafter devised, and include the right to make such modifications as are technically necessary to exercise the rights in other media and formats. If the "Open Access" box has been checked in **Item 1** above, JoVE and the Author hereby grant to the public all such rights in the Article as provided in, but subject to all limitations and requirements set forth in, the CRC License.

4. **Retention of Rights in Article.** Notwithstanding the exclusive license granted to JoVE in **Section 3** above, the Author shall, with respect to the Article, retain the non-exclusive right to use all or part of the Article for the non-commercial purpose of giving lectures, presentations or teaching classes, and to post a copy of the Article on the Institution's website or the Author's personal website, in each case provided that a link to the Article on the JoVE website is provided and notice of JoVE's copyright in the Article is included. All non-copyright intellectual property rights in and to the Article, such as patent rights, shall remain with the Author.

5. **Grant of Rights in Video – Standard Access.** This **Section 5** applies if the "Standard Access" box has been checked in **Item 1** above or if no box has been checked in **Item 1** above. In consideration of JoVE agreeing to produce, display or otherwise assist with the Video, the Author hereby acknowledges and agrees that, Subject to **Section 7** below, JoVE is and shall be the sole and exclusive owner of all rights of any nature, including, without limitation, all copyrights, in and to the Video. To the extent that, by law, the Author is deemed, now or at any time in the future, to have any rights of any nature in or to the Video, the Author hereby disclaims all such rights and transfers all such rights to JoVE.

6. **Grant of Rights in Video – Open Access.** This **Section 6** applies only if the "Open Access" box has been checked in **Item 1** above. In consideration of JoVE agreeing to produce, display or otherwise assist with the Video, the Author hereby grants to JoVE, subject to **Section 7** below, the exclusive, royalty-free, perpetual (for the full term of copyright in the Article, including any extensions thereto) license (a) to publish, reproduce, distribute, display and store the Video in all forms, formats and media whether now known or hereafter developed (including without limitation in print, digital and electronic form) throughout the world, (b) to translate the Video into other languages, create adaptations, summaries or extracts of the Video or other Derivative Works or Collective Works based on all or any portion of the Video and exercise all of the rights set forth in (a) above in such translations, adaptations, summaries, extracts, Derivative Works or Collective Works and (c) to license others to do any or all of the above. The foregoing rights may be exercised in all media and formats, whether now known or hereafter devised, and include the right to make such modifications as are technically necessary to exercise the rights in other media and formats. For any Video to which this **Section 6** is applicable, JoVE and the Author hereby grant to the public all such rights in the Video as provided in, but subject to all limitations and requirements set forth in, the CRC License.

7. **Government Employees.** If the Author is a United States government employee and the Article was prepared in the course of his or her duties as a United States government employee, as indicated in **Item 2** above, and any of the licenses or grants granted by the Author hereunder exceed the scope of the 17 U.S.C. 403, then the rights granted hereunder shall be limited to the maximum rights permitted under such statute. In such case, all provisions contained herein that are not in conflict with such statute shall remain in full force and effect, and all provisions contained herein that do so conflict shall be deemed to be amended so as to provide to JoVE the maximum rights permissible within such statute.

8. **Protection of the Work.** The Author(s) authorize JoVE to take steps in the Author(s) name and on their behalf if JoVE believes some third party could be infringing or might infringe the copyright of either the Author's Article and/or Video.

9. **Likeness, Privacy, Personality.** The Author hereby grants JoVE the right to use the Author's name, voice, likeness, picture, photograph, image, biography and performance in any way, commercial or otherwise, in connection with the Materials and the sale, promotion and distribution thereof. The Author hereby waives any and all rights he or she may have, relating to his or her appearance in the Video or otherwise relating to the Materials, under all applicable privacy, likeness, personality or similar laws.

10. **Author Warranties.** The Author represents and warrants that the Article is original, that it has not been published, that the copyright interest is owned by the Author (or, if more than one author is listed at the beginning of this Agreement, by such authors collectively) and has not been assigned, licensed, or otherwise transferred to any other party. The Author represents and warrants that the author(s) listed at the top of this Agreement are the only authors of the Materials. If more than one author is listed at the top of this Agreement and if any such author has not entered into a separate Article and Video License Agreement with JoVE relating to the Materials, the Author represents and warrants that the Author has been authorized by each of the other such authors to execute this Agreement on his or her behalf and to bind him or her with respect to the terms of this Agreement as if each of them had been a party hereto as an Author. The Author warrants that the use, reproduction, distribution, public or private performance or display, and/or modification of all or any portion of the Materials does not and will not violate, infringe and/or misappropriate the patent, trademark, intellectual property or other rights of any third party. The Author represents and warrants that it has and will continue to comply with all government, institutional and other regulations, including, without limitation all institutional, laboratory, hospital, ethical, human and animal treatment, privacy, and all other rules, regulations, laws, procedures or guidelines, applicable to the Materials, and that all research involving human and animal subjects has been approved by the Author's relevant institutional review board.

11. **JoVE Discretion.** If the Author requests the assistance of JoVE in producing the Video in the Author's facility, the Author shall ensure that the presence of JoVE employees, agents or independent contractors is in accordance with the relevant regulations of the Author's institution. If more than one author is listed at the beginning of this Agreement, JoVE may, in its sole

discretion, elect not take any action with respect to the Article until such time as it has received complete, executed Article and Video License Agreements from each such author. JoVE reserves the right, in its absolute and sole discretion and without giving any reason therefore, to accept or decline any work submitted to JoVE. JoVE and its employees, agents and independent contractors shall have full, unfettered access to the facilities of the Author or of the Author's institution as necessary to make the Video, whether actually published or not. JoVE has sole discretion as to the method of making and publishing the Materials, including, without limitation, to all decisions regarding editing, lighting, filming, timing of publication, if any, length, quality, content and the like.

12. **Indemnification.** The Author agrees to indemnify JoVE and/or its successors and assigns from and against any and all claims, costs, and expenses, including attorney's fees, arising out of any breach of any warranty or other representations contained herein. The Author further agrees to indemnify and hold harmless JoVE from and against any and all claims, costs, and expenses, including attorney's fees, resulting from the breach by the Author of any representation or warranty contained herein or from allegations or instances of violation of intellectual property rights, damage to the Author's or the Author's institution's facilities, fraud, libel, defamation, research, equipment, experiments, property damage, personal injury, violations of institutional, laboratory, hospital, ethical, human and animal treatment, privacy or other rules, regulations, laws, procedures or guidelines, liabilities and other losses or damages related in any way to the submission of work to JoVE, making of videos by JoVE, or publication in JoVE or elsewhere by JoVE. The Author shall be responsible for, and shall hold JoVE harmless from, damages caused by lack of sterilization, lack of cleanliness or by contamination due to the making of a video by JoVE its employees, agents or independent contractors. All sterilization, cleanliness or decontamination procedures shall be solely the responsibility of the Author and shall be undertaken at the Author's expense. All indemnifications provided herein shall include JoVE's attorney's fees and costs related to said losses or damages. Such indemnification and holding harmless shall include such losses or damages incurred by, or in connection with, acts or omissions of JoVE, its employees, agents or independent contractors.

13. **Fees.** To cover the cost incurred for publication, JoVE must receive payment before production and publication of the Materials. Payment is due in 21 days of invoice. Should the Materials not be published due to an editorial or production decision, these funds will be returned to the Author. Withdrawal by the Author of any submitted Materials after final peer review approval will result in a US$1,200 fee to cover pre-production expenses incurred by JoVE. If payment is not received by the completion of filming, production and publication of the Materials will be suspended until payment is received.

14. **Transfer, Governing Law.** This Agreement may be assigned by JoVE and shall inure to the benefits of any of JoVE's successors and assignees. This Agreement shall be governed and construed by the internal laws of the Commonwealth of Massachusetts without giving effect to any conflict of law provision thereunder. This Agreement may be executed in counterparts, each of which shall be deemed an original, but all of which together shall be deemed to me one and the same agreement. A signed copy of this Agreement delivered by facsimile, e-mail or other means of electronic transmission shall be deemed to have the same legal effect as delivery of an original signed copy of this Agreement.